Journal of Innate Immunity

Research Article

J Innate Immun 2023;15:297–316
DOI: 10.1159/000527008

Received: July 10, 2022
Accepted: September 8, 2022
Published online: November 15, 2022

IRF1 Is Required for MDA5 (IFIH1) Induction by IFN-α, LPS, and poly(I:C) in Murine Macrophages

Iris Aparici-Herraiz Guillem Sánchez-Sánchez Carlos Batlle Pere Rehues Martí López-Serrat Lorena Valverde-Estrella Jorge Lloberas Antonio Celada

Macrophage Biology Group, Department of Cellular Biology, Physiology and Immunology, Universitat de Barcelona, Barcelona, Spain

Keywords
Macrophages · Interferons · Gene regulation · Inflammation · Reactive oxygen species

Abstract
Melanoma differentiation-associated protein 5 (MDA5) induces type I interferons (IFNs) after the recognition of viral RNA. In addition, gain-of-function mutations in the interferon induced with helicase C domain 1 (*IFIH1*) gene, which encodes MDA5, lead to type I interferonopathies. Here, we show that *Mda5* is highly expressed in murine macrophages and is regulated by pro-inflammatory stimuli such as the cytokines IFN-α and IFN-γ, the TLR ligand LPS, and a mimic of dsRNA, poly(I:C). *Mda5* induction is mediated through the production of reactive oxygen species. The induction by IFN-α or LPS occurs at the transcriptional level since the *Mda5* mRNA half-life before and after induction is very stable. Interestingly, STAT1 is required for *Mda5* induction by IFN-α, LPS, or poly(I:C). The time course of induction of at least 3 h and the need for protein synthesis indicate that *Mda5* requires an intermediate protein for transcription. In transient transfection experiments, we found that a 105-bp fragment of this gene, between −1153 and −1258 bp relative to the transcription start site, is required for transcription. In this specific region, we observed a sequence containing an IRF-binding motif, which, when mutated, abolishes the induction of *Mda5*. This sequence is strongly conserved in the *IFIH1* promoters of eutherian mammals and in other distant species. Kinetic experiments, chromatin immunoprecipitation assays, and gene-silencing experiments revealed that IRF1 is required for induction of *Mda5* expression.

Introduction

Melanoma differentiation-associated protein 5 (MDA5) is part of the RIG-I-like receptor family and is an important cytosolic sensor of viral RNA, inducing the production of type I interferons (IFNs) [1–4]. MDA5 plays a critical role in viral infections such as those caused by HIV [5, 6] and SARS-CoV-2 [7, 8].

Mda5-deficient mice exhibited a selectively impaired response to several viruses including encephalomyocarditis picornavirus [9, 10], norovirus-1 [11], paramyxoviri-

Jorge Lloberas and Antonio Celada have equally contributed and share senior authorship.

Karger@karger.com
www.karger.com/jin

Correspondence to:
Jorge Lloberas, jlloberas@ub.edu
Antonio Celada, acelada@ub.edu

dae [12, 13], Theiler's encephalomyelitis virus [14], acute lymphocytic choriomeningitis virus [15], or Pichinde virus [16]. Interestingly, the absence of Mda5 protects mice from malaria *plasmodium yoelii* [17]. When infected with encephalomyocarditis virus, mice lacking just one copy of Mda5 developed transient hyperglycemia, whereas homozygous $Mda5^{-/-}$ mice developed severe cardiac pathology [18]. Also, Mda5 is required for a type I IFN response that directly links antigen presentation by dendritic cells (DCs) to adaptive immunity [19], as well as is essential for establishing CD8 T-cell memory [20].

MDA5 contains two domains, the DExD/H-box RNA helicase and a C-terminal domain, that are required for RNA binding [3]. In addition, there are two N-terminal caspase activation and recruitment domains (CARDs) that, after sensing viral RNA, interact with the adapter mitochondrial antiviral-signaling protein (MAVS), ultimately leading to the transcription of the genes encoding type I IFNs [21, 22]. Furthermore, tripartite interaction motif 40 (TRIM40) interacts with caspase activation and recruitment domains and promotes K27- and K48-linked polyubiquitination via its E3 ligase activity, leading to its proteasomal degradation [23]. Dephosphorylation of MDA5 is mediated by the PP1α and PP1γ phosphatases and is essential for its activation [24].

The interaction of MDA5 with MAVS depends on a dynamic balance between phosphorylation and dephosphorylation. Phosphorylation of MDA5 at Ser-828 by RIO kinase 3 inhibits the MDA5 multimer formation required for MAVS activation [25, 26]. Through interactions with TNF receptor-associated factor 6 (TRAF6), tripartite motif protein 25 (TRIM25) is required for the activation of NF-κB and IFN production mediated by MDA5 and MAVS [27]. Type I IFNs induce many genes, including several with antiviral functions as well as the interferon induced with helicase C domain 1 (*IFIH1*) gene encoding MDA5 [2]. Finally, the activation of apoptosis by MAVS induces the removal of the infected cell [28].

Type I interferonopathies are caused by disturbances in intracellular nucleic acid metabolism or in cytosolic nucleic acid sensing pathways that induce an overproduction of type I IFNs, triggering autoimmunity [29]. Cytosolic nucleic acid sensors such as cyclic GMP–AMP synthase and MDA5 recognize broken intracellular self-DNA or RNA produced by high concentrations of several molecules such as reactive oxygen species (ROS) [30], resulting in the production of type I IFNs. Gain-of-function mutations in the *IFIH1* gene are associated with type I interferonopathies, in which type I IFNs are detectable in the cerebrospinal fluid and peripheral blood [29, 31]. *IFIH1* mutations produce Aicardi–Goutières syndrome (AGS) and Singleton-Merten syndrome. AGS is characterized by an early onset of progressive brain disease associated with brain calcifications. The main features of Singleton–Merten syndrome include tooth abnormalities with gum infections, calcifications in the aorta artery and in certain valves of the heart, osteoporosis, and neurological problems. In both syndromes, many symptoms overlap with those of systemic lupus erythematosus. Mutations in the *IFIH1* gene result in a substitution of one amino acid in the helicase domain, producing an MDA5 protein that is a strong inductor of IFN-β in the absence of exogenous stimuli [31, 32].

Single-nucleotide polymorphisms in the *IFIH1* gene have been associated with autoimmune diseases such as type 1 diabetes [33], psoriasis, rheumatoid arthritis, vitiligo, multiple sclerosis, and systemic lupus erythematosus [34, 35]. These *IFIH1* risk alleles may induce augmented levels of the MDA5 protein, increasing responses to RNA derived from cellular sources or viral infections or inducing changes in the conformation of MDA5 that make it constitutively active [36, 37]. It is likely that all these mechanisms involve a chronic induction of type I IFNs, which then initiates or increases autoimmune responses.

Recently, it has been reported that RNAs accumulate during cancer treatment with DNA-demethylating agents, inducing MDA5 activation. The production of type I IFNs results in reduced cell growth and self-renewal [38, 39]. Finally, when mitochondrial RNA degradation is impaired, dsRNA escapes into the cytosol and activates MDA5, which subsequently leads to the production of type I IFNs [40].

Although a large number of the negative regulators of the RIG-I-like receptor signaling pathway have been described [41], the role of transcriptional regulation has not been reported to date. Here, we report that MDA5 is highly expressed in macrophages and is induced by pro-inflammatory agents (IFN-α and LPS) and poly(I:C). These activators transcriptionally upregulate *Mda5* expression with the time course of an intermediate gene. This upregulation requires IFN regulatory factor (IRF) 1, which binds to an IRF box in the *Mda5* gene promoter to induce transcription.

Materials and Methods

Reagents

Recombinant murine IFN-γ, IFN-α, TNF-α, IL-4, IL-6, IL-10, and M-CSF were purchased from R&D Systems (Minneapolis, MN). R848 and cpGB were obtained from InvivoGen (San Diego,

CA) and high molecular weight poly(I:C) from Sigma-Aldrich, P1530 (St. Louis, MO). Recombinant M-CSF and GM-CSF were purchased from Pepro Tech (Cranbury, NJ). Actinomycin D, cycloheximide (CHX), LPS (Cat# L3129), 5,6-dichlorobenzimidazole 1-β-D-ribofuranoside (DBR), penicillin, and streptomycin were purchased from Sigma-Aldrich. All the other chemicals were of the highest purity available and were also purchased from Sigma-Aldrich. Deionized water was further purified with a Millipore Milli-Q system Q-POD A10 (Merck KGaA, Darmstadt, Germany). All the restriction enzymes were supplied by Roche (Basel, Switzerland).

Primary Cell Cultures and Cell Lines

Bone marrow-derived macrophages (BMDMs) were isolated from 8-week-old C57BL/6 female mice (Charles River Laboratories, Wilmington, MA, USA), as described previously [42]. Bone marrow cells from the femur, tibia, and humerus were flushed and grown on plastic tissue culture dishes (150 mm) in DMEM (Cultek, Madrid, Spain) containing 20% FCS (GIBCO; Thermo Fisher Scientific, Waltham, MA, USA) and recombinant M-CSF (20 ng/mL). The medium was supplemented with 100 U/mL of penicillin and 100 μg/mL of streptomycin. Cells were incubated at 37°C in a humidified atmosphere with 5% CO_2. After 7 days of culture, a homogeneous population of adherent macrophages was obtained (in 20 independent experiments, macrophages were 99.34 ± 0.52% CD11b/CD18 and 98.41 ± 0.93% F4/80).

Stat1 knockout mice were kindly provided by Dr. Anna Planas (CSIC-IDIBAPS, Spain) [43]. For the experiments with these mice, we used the corresponding co-housed background mouse controls. The animals were kept under specific pathogen-free conditions at the animal facility of the Barcelona Science Park. Animal use was approved by the Animal Research Committee of the University of Barcelona and the Government of Catalonia (approval number 2523). The RAW 264.7 macrophage cell line (American Type Culture Collection, Manassas, VI, USA) was maintained in DMEM supplemented with 10% heat-inactivated FCS, 100 U/mL of penicillin and 100 μg/mL of streptomycin.

DCs were obtained from BMDM as described [44]. To differentiate into DCs, bone marrow cells were cultured in DMEM, 10% FCS, and 5 ng/mL GM-CSF. On days 2 and 4, the plates were shaken and the culture supernatant was collected and replaced by fresh medium with GM-CSF. On days 6 and 8, plates were fed aspirating supernatants (without shaking) and medium with GM-CSF was added. On day 8, cells were stimulated with 1 μg/mL LPS for 48 h. On day 10, the plates were shaken, the supernatant was collected, and DCs were separated from adherent macrophages.

Transfections

To introduce poly(I:C) into the BMDMs, the electroporation technique was used. Electroporation was carried out with the Neon Transfection System (Thermo Fisher; Cat. No. MPK5000, Waltham, MA, USA), following the manufacturer's instructions. For each experiment, we used 10^6 macrophages (RAW 264.7) suspended in 100 μL of buffer R (supplied with the kit MPK10096, Thermo Fisher) containing 2 μg of poly(I:C). Electroporation was carried out with two pulses at 1,400 V for 20 ms. After electroporation, cells were incubated for the time corresponding to the duration of the stimulus (from 1 h to 24 h). For control, a set of cells suspended in buffer R and poly(I:C) was also used, but without electroporation. For the RAW 264.7 cell line, intracellular stimulation with poly(I:C) was carried out using the SuperFect transfection reagent (Qiagen, Germantown, MD, USA), following the manufacturer's instructions.

RNA Extraction, Reverse Transcription PCR, and Quantitative PCR

RNA extraction was performed as described previously [45]. Briefly, total RNA from cells was extracted and purified using the ReliaPrep RNA Miniprep System (Promega, Madison, WI, USA) for PCR and to clone the reporter plasmids. For quantitative PCR (qPCR), RNA was extracted using the Maxwell® automatic system and the Maxwell® 16 LEV simplyRNA Purification Kit from Promega. RNA was treated with DNAse (Roche) to remove contaminating DNA before being retrotranscribed into cDNA using the Moloney murine leukemia virus reverse transcriptase, RNase H Minus (Promega), following the manufacturer's indications. qPCR was performed using the SYBR Green Master Mix (Applied Biosystems, Waltham, MA, USA). Primers were designed using Primer3Plus (https://www.bioinformatics.nl/cgi-bin/primer3plus/primer3plus.cgi). As a negative control for each gene, water was used. When a signal was detected in these negative controls (at 40 Ct), the primer pairs used were discarded and replaced with alternative ones for the same gene. Furthermore, the amplification efficiency for each pair of primers was calculated by making a standard curve from serially diluted cDNA samples. Only the primer pairs with an amplification efficiency of 100 ± 10% were used. The list of primers (Sigma-Aldrich) can be found in Table 1. The data were analyzed with the ΔΔCt method [46], using the Biogazelle Qbase + software. Gene expression was normalized to that of three reference genes (i.e., housekeeping genes): *Hprt1*, *L14*, and *Sdha*. The stability of these reference genes was determined by ensuring that their geNorm M value was lower than 0.5 [47].

Western Blot Analysis

Total cytoplasmic extracts were obtained by lysing cells, as described previously [30]. SDS-PAGE was performed and the gels were transferred onto nitrocellulose membranes (Hybond-C, Amersham Biosciences, UK). After blocking with dry milk for 1 h, the membranes were incubated with the rabbit polyclonal anti-MDA5 (IFIH1) antibody (Proteintech 21775-1-AP, Rosemont, PE, USA) diluted 1:250 in Tris-buffered saline (TBS, Thermo Fisher) containing 0.1% Tween 20 (Sigma-Aldrich) overnight at 4°C. The membranes were then incubated with the secondary antibody, a goat anti-rabbit IgG (H + L)-HRP antibody diluted 1:2,000 (Jackson ImmunoResearch 111-035-003, West Grove, PA, USA), for 1 h at room temperature (RT). β-actin was used as the loading control and was detected using a mouse anti-β-actin antibody (Sigma-Aldrich A5441; diluted 1:5,000). The secondary antibody used was a rabbit anti-mouse IgG-HRP antibody (Sigma-Aldrich A9044; diluted 1:5,000). Detection was performed using ECL (Amersham) and the membrane was exposed to X-ray films (Agfa, Mortsel, Belgium).

Transfection of Small Interfering RNA

We used the online tool MWG Eurofins (Ebersberg, Germany) to inhibit IRF1 expression, which was performed as described previously [48]. We used a mixture of three specific oligonucleotides for IRF1 (UCACUCGAAUGCGGAUG, GGAUCAGAGUAGGAACA, and UCAGAGGUGUACACUAA) and a control oligonucleotide directed against a sequence not present in macrophages (green

Table 1. List of the primers used in qPCR

Gene	NCBI reference	Forward primer (5′ to 3′)	Reverse primer (5′ to 3′)
Mda5 (Ifih1)	71586	GCCTGGAACGTAGACGACAT	TGGTTGGGCCACTTCCATTT
Ifn-β	15977	CAGCTCCAAGAAAGGACGA	GGCAGTGTAACTCTTCTGCA
Rig-I	230073	GGCTGAAAGCAAGGCTGATG	ACGCTATCAGATGTTGCCCC
Irf1	16362	GAGATGTTAGCCCGGACACTTT	CCATATCCAAGTCCTGACCCA
Irf3	54131	GAGAGCCGAACGAGGTTCAG	CTTCCAGGTTGACACGTCCG
Irf7	54123	CCCCAGCCGGTGATCTTTC	CACAGTGACGGTCCTCGAAG
Irf8	15900	TGACACCAACCAGTTCATCCGAGA	CACCAGAATGAGTTTGGAGCGCAA
Irf9	16391	GCCGAGTGGTGGGTAAGAC	GCAAAGGCGCTGAACAAAGAG
c-myc	17869	AACAGCTTCGAAACTCTGGTGC	CGCATCAGTTCTGTCAGAAGGA
Arginase 1	11846	TTGCGAGACGTAGACCCTGG	CAAAGCTCAGGTGAATCGGC
Tnf-α	21926	CCAGACCCTCACACTCAGATC	CACTTGGTGGTTTGCTACGAC
L14	68463	TCCCAGGCTGTTAACGCGGT	GCGCTGGCTGAATGCTCTG
Hprt	15452	ATCATTATGCCGAGGATTTGG	GCAAAGAACTTATAGCCCCC
Sdha	66945	TGGGGAGTGCCGTGGTGTCA	CATGGCTGTGCCGTCCCCTG

Primers were chosen based on their position regarding genomic sequence and, to avoid unspecific genomic DNA amplification, should be localized at a distance of 1 or more introns. Primers were designed using at the online Primer-Blast (NCBI).

Table 2. Oligonucleotides used in the cloning of different plasmids

Name	Sequence (5′ to 3′)
pCR2.1−1481 forward	AACGCTGTCACGAGGTTCAT
pCR2.1+384 reverse	TTTGTCCACCAAAGTGGGCT
pGL3−1481 forward	GGTACCGAGCTCAACGCTGTCACGAGGTTCAT
pGL3+384 reverse	TTACCGTTCGAATTTGTCCACCAAAGTGGGCT
pGL·box 1 upstream forward	CTATCGATAGGTACCGAGCTCAACGCTGTCACGAGGTTCA
pGL·box 1 upstream reverse	GAGGAACATTATCAGATAGTCACGTTTAGAAAAATTAATCTTTTAG
pGL·box 1 downstream forward	ACTATCTGATAATGTTCCTCCATAGCTGGTG
pGL·box 1 downstream reverse	CCAACAGTACCGGAATGCCATTTTGTCCACCAAAGTGGGC
pGL·box 2 upstream forward	CTATCGATAGGTACCGAGCTGGTACCGAGCTCAACGCTGTCAC
pGL·box 2 upstream reverse	TAATAGGGAGTCCAGACCTCCAGGGGGCGT
pGL·box 2 downstream forward	GAGGTCTGGACTCCCTATTAACTGACAAGTG
pGL·box 2 downstream reverse	GGTGGCTTTACCAACAGTAC
pGL·box 3 upstream forward	CTATCGATAGGTACCGAGCTGGTACCGAGCTCAACGCTGT
pGL·box 3 upstream reverse	TCGCTCTGCGAAGTTTCGTGAGGGTGGAGG
pGL·box 3 downstream forward	CACGAAACTTCGCAGAGCGAGAGCGGTCCC
pGL·box 3 downstream reverse	GGTGGCTTTACCAACAGTACCGGAATG
Mutated box 3 upstream forward	CCCCCCCCAGAACATTTCTCTATCG
Mutated box 3 upstream reverse	CAGATCGGCCCCTGCCCCGATTCTC
Mutated box 3 downstream forward	GAGAATCGGGGCAGGGGCCGATCTG
Mutated box 3 downstream reverse	GGGGGGGTGGCTTTACCAACAGTACCG
Fragment mutation upstream forward	CCCCCAGAACATTTCTCTATCG
Fragment mutation upstream reverse	ACAGTACCGGAATGCCAAGC

fluorescent protein: GGCUACGUCCAGGAGCGCACC). Transfection of 0.2 μM of each small interfering RNA (siRNA) was carried out by electroporation, as described for poly(I:C) with the Neon Transfection System. After electroporation, cells were incubated for 0, 6, and 24 h in 6-well plates in 3 mL of media (50% DMEM supplemented with 20% FBS and 30% L-cell conditioned media containing 100 U/mL of penicillin and 100 μg/mL of streptomycin).

Reporter Plasmids

The *Mda5* promoter region was cloned from genomic DNA extracted from 10^7 BMDMs. This 1865-bp region (−1481 to +384 bp) was amplified by PCR (pCR2.1−1481 forward, pCR2.1+384 reverse (Table 2)); and cloned into the pCR2.1 plasmid (Thermo Fisher). Then, we generated restriction sites for *SacI* and *HindIII* at the extremes of the *Mda5* fragment using the primers pGL3−1481

forward and pGL3+384 reverse (Table 2), which allowed the insertion of pGL3-BASIC (Promega) into the multicloning site, following the manufacturer's instructions for the pGL3-1865 vector. Next, using the pGL3-1865 vector, we made the deletions of boxes 1, 2, or 3. The primers were designed using the NEBuilder Assembly Tool (New England BioLabs, Ipswich, MA, USA) (Table 2) and were used to amplify the fragments flanking (above and below) the box that was to be deleted using the Kit Expand High Fidelity PCR System (Roche). Once the fragments were amplified, we ligated the two fragments and the empty pGL3 vector opened at restriction sites *SacI* and *HindIII* using the NEBuilder HiFi DNA Assembly Master Mix (New England BioLabs). The vectors generated were pGL3-box 1 deleted, pGL3-box 2 deleted, and pGL3-box 3 deleted.

The pGL3-1865 plasmid was used as a template in PCR-directed mutagenesis. Two pairs of primers were designed in order to introduce the mutation at the site of interest (Table 2). Among the first pair of primers, the forward primer (mutated box 3 upstream forward) bound to the vector near the 5′ end of the *Mda5* promoter, while the reverse primer (mutated box 3 upstream reverse), containing the mutation, targeted the IRF1 binding sequence. The PCR product obtained from this primer pair was called the mutated box 3 upstream fragment (1246 bp). Among the second pair of primers, the forward primer (mutated box 3 downstream forward), with the mutated base pairs, targeted the IRF1 binding sequence, while the reverse primer (mutated box 3 downstream reverse) hybridized with the vector near the 3′ end of the promoter. The PCR product obtained from this primer pair was called the mutated box 3 downstream fragment (724 bp).

The PCR-mediated recombination was performed using both the mutated box 3 upstream and downstream fragments as templates. A new pair of primers was used, fragment mutation upstream forward and fragment mutation upstream reverse, targeting the 5′ end of the upstream fragment and the 3′ end of the downstream fragment, respectively. The plasmid obtained was called pGL3-box 3 mutated. All the primers were purchased from Sigma-Aldrich.

All the plasmids were sequenced using Big Dye 3.1 from PerkinElmer (Wellesley, MA) and the following primers: the forward primer 5′-CCTCTTCGCTATTACGCCAG-3′ and the reverse primer 5′-ACCCCTTTTTGGAAACGAAC-3′; and the forward primer 5′-ACAGGGACCTTGCATACTGG-3′ and the reverse primer 5′-GGAGAGGGCAGATCAGTGAG-3'. These primers were designed using MacVector version 12.5.1 (MacVector Inc, Cary, NC, USA).

Transient Transfection and Dual-Luciferase Reporter Assays

For plasmid transfection, 10^5 RAW 264.7 cells were seeded in 24-well plates in 1 mL of DMEM with 10% FCS. Cells were co-transfected with a Renilla luciferase-expressing plasmid to verify the uniformity of the transfection. Transfection of 1 μg of plasmid DNA (pGL3 constructs and pRL-TK-Renilla at a 100:1 ratio) per well was carried out using 7.5 μL of the *Superfect* tranfection reagent (Quiagen, Germantown, MA, USA), following the manufacturer's instructions. Eighteen hours later, cells were stimulated with IFN-γ, IFN-α, LPS, or poly(I:C) for 1–24 h (as specified) or left untreated. Firefly luciferase and Renilla luciferase activities were determined using the Promega Dual-Luciferase Reporter Assay System and a TD-20/20 luminometer (Turner Designs, San Jose, CA, USA), following the manufacturers' instructions.

Chromatin Immunoprecipitation Assays

The chromatin immunoprecipitation (ChIP) assays were performed as described previously [49]. After incubation with LPS, IFN-α, or poly(I:C) for 24 h, 20×10^6 BMDMs were cultured in a 150-mm plate and fixed in paraformaldehyde. After 10 min at RT and under gentle agitation, glycine (2 M solution) was added to stop the fixation. After 5 min, the plates were washed two times with 10 mL of cold PBS, and the BMDMs were then scraped and recovered in 0.1 M Tris-HCl, pH 9.4, containing 10 mM DTT. The recovered cells were incubated for 15 min at 30°C and then centrifuged at 800 g for 5 min at 4°C. The precipitate was then resuspended and centrifuged in 1 mL of PBS, buffer I (10 mM HEPES, pH 6.5, 0.25% Triton X-100, 10 mM EDTA, and 0.5 mM EGTA) and, after that, in buffer II (10 mM HEPES, pH 6.5, 20 mM NaCl, 1 mM EDTA, and 0.5 mM EGTA). Before the centrifugation, a protease inhibitor cocktail (1 mM PMSF, 1 mM iodoacetamide, 1 mM sodium orthovanadate, 10 μg/mL of aprotinin, and 1 μg/mL of leupeptin) was added to the three solutions. Finally, the cells were resuspended in 300 μL of lysis buffer (1% SDS, 10 mM EDTA, 0.5 mM Tris-HCl, pH 8.1, and the protease inhibitor cocktail) at RT. After that, the samples were sonicated using Bioruptor Twin (Diagenode; Liege, Belgium) for 10 min at the high mode (30" on/30" off). The procedure was repeated 5 times. Following this, a DNA agarose gel electrophoresis was performed to confirm a good sonication of the samples (a large number of the DNA fragments should have a size of 200 bp to 1200 bp). The resulting soluble chromatin was centrifuged at 16,000 *g* for 10 min and diluted in the dilution buffer (1% Triton X-100, 2 mM EDTA, 150 mM NaCl, and 20 mM Tris-HCl, pH 8.1, and a protease inhibitor cocktail) to a final volume of 1.1 mL. At that moment, 100 μL was separated and stored at 4°C to be used as control or INPUT. To reduce nonspecific interactions, the remaining sample was preincubated with 2 μg of sonicated salmon sperm DNA (Amersham), 2.6 μg of nonspecific IgGs (Sigma-Aldrich), and 20 μg of Magna ChIP protein A magnetic beads (Millipore, Burlington, MA, USA) overnight at 4°C. The sample was then centrifuged at 16,000 *g* for 10 s to remove the beads, before being diluted again to obtain a final volume of 2 mL (1 mL for the specific precipitate and 1 mL for the control precipitate). The two precipitates were incubated for 6 h with an identical concentration of the anti-IRF1 antibody (sc-514544, Santa Cruz Biotechnology, Santa Cruz, CA; diluted 1:250) or a nonspecific IgG, respectively. After that, the samples were incubated overnight at 4°C with 20 μL of magnetic beads. The next day, the samples were centrifuged (16,000 *g* for 10 s) and the remaining beads were sequentially washed and incubated for 10 min in 1 mL of TSE I (150 mM NaCl, 0.1% SDS, 1% Triton X-100, 2 mM EDTA, and 20 mM Tris-HCl, pH 8.1), 1 mL of TSE II (500 mM NaCl, 0.1% SDS, 1% Triton X-100, 2 mM EDTA, and 20 mM Tris-HCl, pH 8.1), and 1 mL of buffer III (0.25 M LiCl, 1% NP-40, 1% w/v deoxycholate, 1 mM EDTA, and 10 mM Tris-HCl, pH 8.1). Following this, the beads were washed with 1 mL of PBS (4°C) and the immunoprecipitates were finally eluted with 300 μL of the elution solution (0.1 M NaHCO3 and 1% SDS), which had to be prepared the same day. The elution was performed in three washing steps. First, the beads were incubated in 100 μL of the elution solution for 20 min. After this incubation, the samples were centrifuged at 16,000 *g* for 10 s, with the resulting supernatant recovered in a 1.5-mL Eppendorf tube. This elution procedure was repeated two more times until a final volume of 300 μL was obtained. Before DNA purification, a "reverse crosslinking" step was required. The 300-μL samples

(nonspecific and IRF1 immunoprecipitates) and INPUTs were incubated overnight at 65°C. The next day, the DNA of the samples was purified with the QIAquick PCR Purification Kit (Qiagen), following the manufacturer's instructions, with a final elution volume of 30 µL. The final samples were analyzed by qPCR using the following primers: 5′-TTGTTGAGGGTTTTGTATTGTTG-3′ and 5′-GATGCATGCTGACTTTAGCC-3′ for box 3 of the *Mda5* promoter; and 5′-AGATGCAGCAGATCCGCAT-3′ and 5′-GTTCTTGCCCATCAGCACC-3′ for the control (a non-promoter region of an unrelated gene, the *36B4* gene encoding a ribosomal protein). The design of the primer for *Mda5* box 3 was performed with the online tool Primer3Plus. The final results were obtained after two normalization steps, with the first step involving the specific INPUTs and the second one involving the results obtained from the analysis of a gene located outside the promoter region of *Mda5*.

Statistical Analysis and Databases

Data were analyzed using the nonparametric Mann-Whitney U test when the number of values was at least 4 or the Student's *t* test when the number of values was 3. Statistical analysis was performed with the GraphPad Prism 9 software. In some experiments, we used the JASPAR database (http://jaspar.genereg.net) and the National Center for Biotechnology Information (https://www.ncbi.nlm.nih.gov) database. For sequence alignment, we used MacVector 18.0 (MacVector, North Carolina). Philograms were done with Multiple Sequence Alignment by CLUSTALW (https://www.genome.jp/tools-bin/clustalw). Also, the Ensembl genome browser 106 (https://www.ensembl.org) and the Gene Expression Omnibus (GEO) database (http://www.ncbi.nlm.nih.gov/gds) were used. Evolutionary analyses were conducted in MEGA6 (https://www.ncbi.nlm.nih.gov) [50, 51].

Results

Mda5 Expression in Macrophages Is Regulated by IFN-α, IFN-γ, LPS, and poly(I:C)

We obtained murine BMs and differentiated them in vitro into BMDMs. The resulting homogenous population of cells was composed of quiescent primary macrophages that could be induced to proliferate by growth factors or be classically and alternatively activated by cytokines [52]. To define the anatomical distribution of *Mda5*, we measured the expression of this gene by qPCR in several mouse organs. Several tissues such as the eye, intestine, spleen, pancreas, lung, thymus, liver, adipose, and trachea showed a higher expression of *Mda5* than other tissues such as the skin, brain, tongue, testes, stomach, heart, muscle, kidney, and esophagus (Fig. 1a). We used peritoneal macrophages and BMDMs as a positive control since they had already been reported to express *Mda5* [10, 53].

Macrophages were incubated with pro-inflammatory (IFN-γ, IFN-α, LPS (TLR4), R848 (TLR8/9), CPGB (TLR9), TNF-α and IL-6), anti-inflammatory (IL-4 and IL-10) agents, or the growth factor M-CSF to determine whether the treatment affected *Mda5* expression. After 24 h of incubation with IFN-γ, IFN-α, or LPS, significant changes in *Mda5* expression were observed (Fig. 1b). However, no increased expression was observed with the other stimuli. An increase in *Mda5* expression was detected as a function of time after stimulation with IFN-γ, IFN-α, or LPS. The expression of this gene increased, reaching a maximum within the first 6–9 h of incubation that was about 8 to 4 times the basal expression (Fig. 1c). At 24 h of incubation with IFN-α or LPS, a moderate decrease was observed, but remained significantly increased.

We also analyzed the expression of *Mda5* in peritoneal macrophages and DCs. In both cases, *Mda5* expression increased in response to IFN-α or LPS (Fig. 1d), as has been reported for DCs [13].

The induction of mRNA levels correlated with an increase in protein expression, as confirmed by western blotting (Fig. 2a). The figure shows the expression of a split band around 125Kd compatible with a phosphorylation at both the NH2- and COOH-terminal ends (Ser-88 and Ser-828) as described [24, 26]. In resting macrophages, MDA5 is barely visible, but its levels increased by about 9 and 6 times in response to stimulation with IFN-α and LPS, respectively, but not with IL-4 (Fig. 2b).

Fig. 1. Selective tissue expression of Mda5. **a** Tissues from three mice were used to obtain RNA, and *Mda5* expression was determined by RT-PCR (independent experiments, $n = 3$). For comparison, we used BMDMs and peritoneal macrophages that were significantly increased in relation to all the tissues ($p < 0.01$). **b** Seven-day-old BMDMs were starved of growth factors for 16–18 h and then incubated for 24 h with different stimuli at a concentration of 10 ng/mL with the exception of R848 and CpG which was 2.5 µg/mL. *Mda5* expression was then determined by RT-PCR ($n = 3$). Controls were untreated cells. **c** Time course of *Mda5* expression. BMDMs were incubated with the indicated stimuli, and *Mda5* induction was measured by RT-PCR ($n = 4$). **d** Mda5 expression is induced in BMDM, peritoneal macrophages and DCs by IFN-α or LPS. Cells were incubated for 24 h with the indicated stimuli and *Mda5* expression was then determined by RT-PCR ($n = 3$). Each experiment was performed in triplicate, and the results are shown as the mean ± SD. *$p < 0.05$, **$p < 0.01$, ***$p < 0.001$, and ****$p < 0.0001$ in relation to each stimulated sample compared to controls in each experiment. Data were analyzed using the unpaired Student's *t* test with the exception of **c** that was calculated using a two-way ANOVA test followed by a Bonferroni correction.

(For figure see next page.)

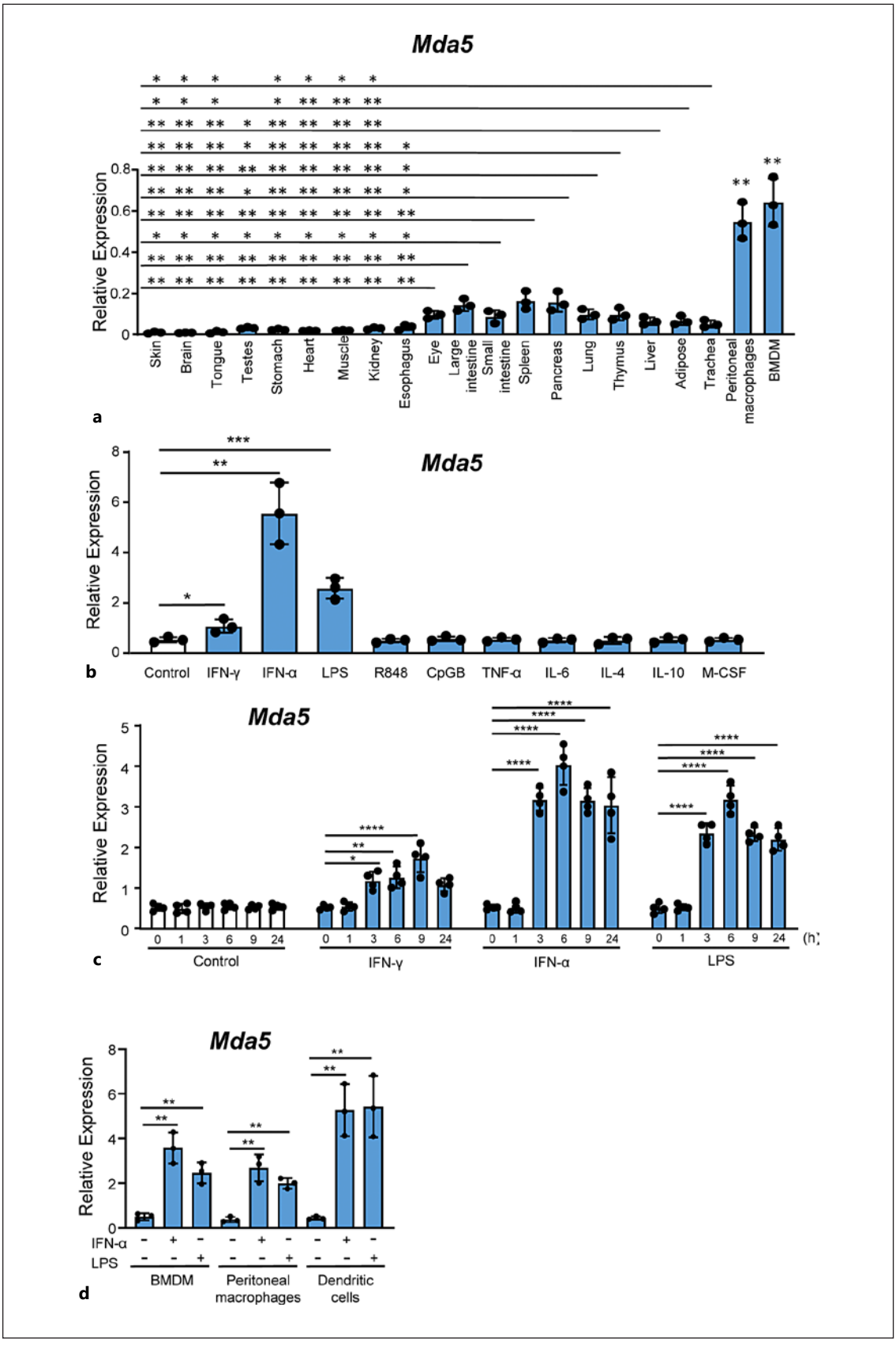
Mda5
Relative Expression
Skin
Brain
Tongue
Testes
Stomach
Heart
Muscle
Kidney
Esophagus
Eye
Large intestine
Small intestine
Spleen
Pancreas
Lung
Thymus
Liver
Adipose
Trachea
Peritoneal macrophages
BMDM
a
Mda5
Relative Expression
Control
IFN-γ
IFN-α
LPS
R848
CpGB
TNF-α
IL-6
IL-4
IL-10
M-CSF
b
Mda5
Relative Expression
0 1 3 6 9 24 (h)
Control
IFN-γ
IFN-α
LPS
c
Mda5
Relative Expression
IFN-α
LPS
BMDM
Peritoneal macrophages
Dendritic cells
d

1

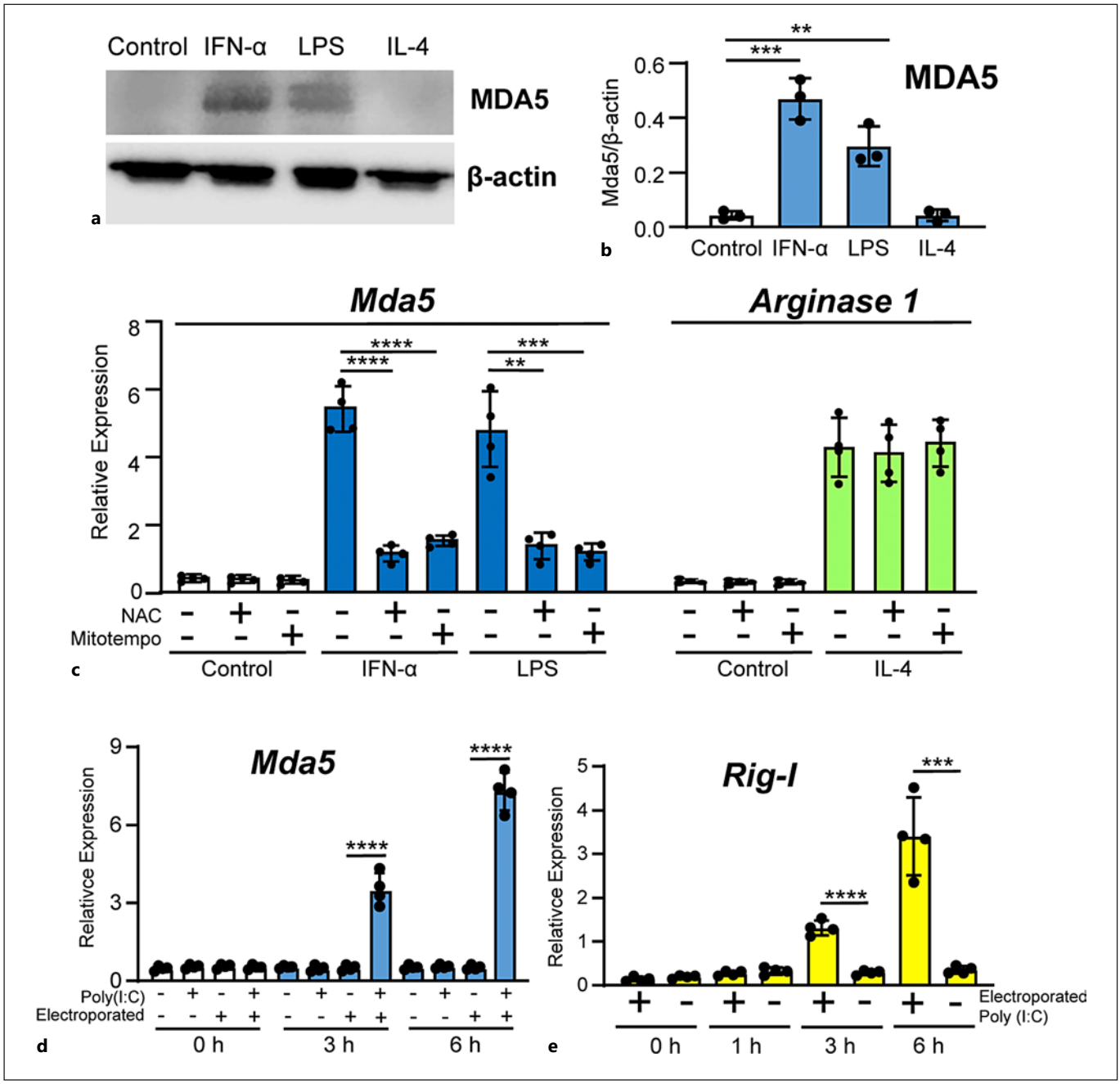

Fig. 2. Protein and mRNA expression of MDA5. **a** Representative blot of MDA5 protein expression in BMDMs. Total protein extracts from BMDMs treated for 24 h with the indicated stimuli were subjected to western blotting to determine MDA5 expression. β-actin was used as the loading control. **b** Quantitation of MDA5 expression in three independent experiments in relation to β-actin expression ($n = 3$). **c** BMDMs were incubated for 1 h with media, NAC (20 mM) or Mito-TEMPO (50 μM). The BMDMs were then treated with IFN-α or LPS for 3h and *Mda5* expression was determined ($n = 4$). As control, BMDMs were treated with IL-4 and *Arginase 1* was determined ($n = 4$). **d** BMDMs were electroporated with poly(I:C) (2 μg in 100 μL), while controls were non-electroporated BMDMs. The mock transfection controls were the electroporated cells with media. *Mda5* expression was determined at the indicated times ($n = 4$). **e** Similar experiment to that in (**d**), but *Rig-I* expression was determined instead ($n = 4$). Each experiment was performed in triplicate, and the results are shown as the mean ± SD. $^{**}p < 0.01$, $^{***}p < 0.001$, and $^{*}p < 0.0001$ in relation to each stimulated sample compared to controls in each experiment. Data were analyzed using the unpaired Student's *t* test.

Macrophages treated for 1 h with the antioxidant N-acetylcysteine (NAC) (which abolishes total cellular ROS) before IFN-α or LPS treatment showed strongly reduced Mda5 expression (Fig. 2c). We also used Mito-TEMPO, a mitochondria-specific ROS scavenger, which caused a dramatic repression of *Mda5* expression (Fig. 2c). As a control, we used the expression of *Arginase 1* that is not affected by ROS scavengers. These results suggested an important role for ROS in the expression of *Mda5*.

Given that MDA5 is an important cytosolic sensor of viral RNA and that it induces the production of type I IFNs [2–4], we used poly(I:C), a synthetic analog of double-stranded RNA [54]. As expected, extracellular high molecular weight poly(I:C) did not induce *Mda5* expression (Fig. 2d). However, electroporated poly(I:C) induced a strong expression of *Mda5* after 3 and 6 h of incubation (Fig. 2d). As a control, we determined poly(I:C)-induced *Rig-I* expression since RIG-I is another sensor of short dsRNA. After 3 h, electroporated poly(I:C) started the induction of *Rig-I* expression (Fig. 2e) [55].

Induction of Mda5 by IFN-α or LPS Is at the Transcriptional Level in Macrophages

To examine whether the increase in *Mda5* expression induced by IFN-α or LPS treatment occurred at the transcriptional level or was due to mRNA stabilization, we determined the half-life of *Mda5* transcripts in cells treated or not with IFN-α or LPS. Macrophages were treated with IFN-α for 6 h to induce *Mda5* expression. Actinomycin D and DBR were then added at a concentration sufficient to block all further mRNA synthesis (5 μg/mL and 20 μg/mL, respectively), which was determined by [^{3H}]UTP incorporation [56]. We then isolated mRNA from these treated macrophages at several time points. Measurement of *Mda5* expression by RT-PCR revealed a stable half-life of its mRNA in the resting cells (Fig. 3a). As a control, the half-life of *c-myc* was measured, which was approximately 48 min [57]. IFN-α treatment did not modify the stability of *Mda5* (Fig. 3a). Similar results were found for LPS (Fig. 3b). These results demonstrated that the mRNA of *Mda5* was very stable under basal conditions and after stimulation. Therefore, if the *Mda5* mRNA level increased in response to several stimuli but its half-life did not increase, this indicated that the induction was at the transcriptional level.

Given that IFN-γ signaling is mediated by STAT1 in most cases [43], we wanted to confirm the involvement of STAT1 in the regulation of *Mda5* expression by IFN-γ. Therefore, we stimulated macrophages from STAT1-deficient mice with IFN-γ for a range of time periods. RNA was then extracted and *Mda5* expression was determined by RT-PCR. In comparison to control cells, the induction of *Mda5* expression in macrophages from STAT1-deficient mice was impaired (Fig. 3c). As expected, similar results were obtained when we used IFN-α (Fig. 3c). The effect of LPS was also dependent on STAT1 (Fig. 3c). This was probably due to a secondary induction of type I IFNs, as has been described for other genes [58, 59]. Remarkably, electroporated macrophages with poly(I:C) also required STAT1 to induce the expression of *Mda5* (Fig. 3d). These observations confirmed a critical role for STAT1 in the induction of *Mda5* expression by the activators used.

We noticed that the induction of *Mda5* in macrophages required at least 3 h (Fig. 1c), suggesting that during the time between the receptor-ligand binding and the transcription, other events in addition to STAT1 activation may also be required. Therefore, as a control, we tested the induction of *Ifn-β* by IFN-γ and its dependence on STAT1 activation. *Ifn-β* induction was rapid, occurring in about 1 h, and was dependent on STAT1 activation (Fig. 3e) [43]. *Mda5* expression was induced after 3 h of treatment with the different activators (Fig. 1c, 2d), suggesting the need for protein synthesis to induce Mda5. The inhibition of protein synthesis by CHX treatment prevented the activation of *Mda5* expression (Fig. 3f). CHX treatment alone did not elicit Mda5 expression. As a control, we used the LPS-induced *Tnf-α*, an early gene that does not require protein synthesis [56] (Fig. 3g). These results demonstrated that after STAT1 activation, de novo protein synthesis was necessary for inducing *Mda5* expression [60].

Functional Analysis of the Promoter in Mda5 Induction

Given the difficulties in transfecting non-transformed cells, particularly macrophages, we studied whether the RAW 264.7 macrophage cell line could be used for a functional analysis of the *Mda5* promoter. Incubation of these cells with IFN-α, LPS, or poly(I:C) for various periods of time induced *Mda5* expression with similar kinetics as those shown by BMDMs (Fig. 4a, b).

We then examined the kinetics of the expression of a fragment of the promoter (−1481 to +384 bp) that was linked to a luciferase. This vector (pGL3-1865) was transfected into RAW 264.7 macrophages, and luciferase activity was measured. Each construct was co-transfected with the Renilla luciferase-expressing vector to correct for any differences in transfection efficiency. All luciferase activity values were normalized to the level of the Renilla luciferase expression. RAW 264.7 macrophages were

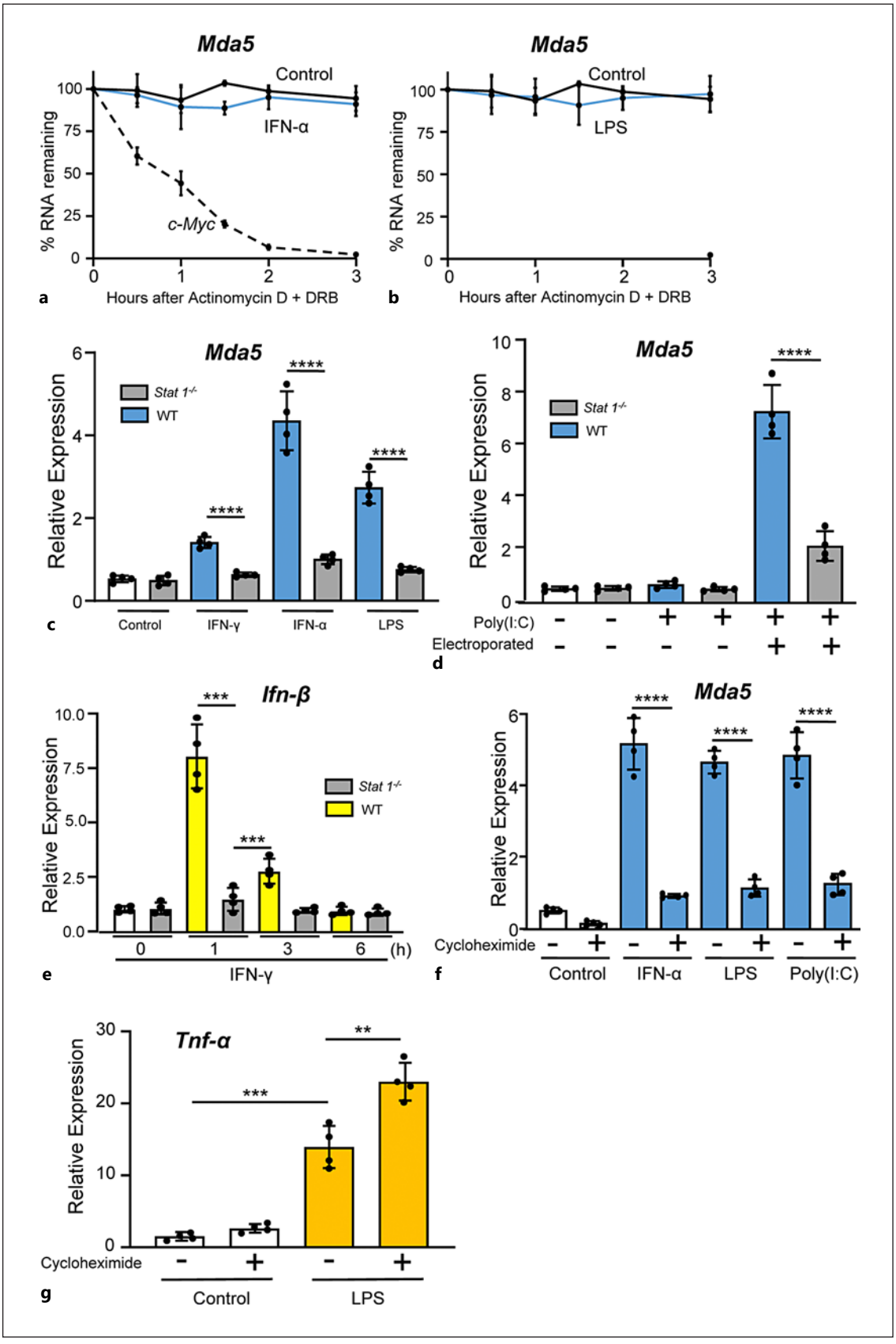

3

(For legend see next page.)

treated with LPS or IFN-α. At 6 h of treatment, the expression of this fragment showed a significant increase in a time-dependent manner (Fig. 4c). However, almost no induction was observed in non-treated cells with the activators.

To determine the putative elements responsible for the transcriptional regulation of *Mda5*, the 1865-bp promoter fragment was studied using the JASPAR database. We identified three putative regulatory areas located at −1333 bp to −1283 bp (box 1), −1153 bp to −1268 bp (box 2), and −328 bp to −213 bp (box 3) (Fig. 4d) that contained putative sequences for transcription factor binding. To determine the possible transcriptional activity of these sequences, we deleted these areas in the pGL3-1310 vector (Fig. 4d) and determined the effect on transcriptional activity. Luciferase activity was induced only when we treated the macrophages with LPS, IFN-α, or poly(I:C) (Fig. 4d). Elimination of boxes 1 or 2 did not modify the amount of luciferase activity in relation to the control. However, deletion of box 3 completely abolished the activity (Fig. 4d), suggesting that this region is important for the transcriptional regulation of *Mda5*.

Analysis of the 5′-proximal regions of *Mda5* revealed the absence of the canonical TATA and CCAAT boxes. However, there is an AAGAGAATCGAAACAGAAAC sequence located at −306 to −286 in relation to the ATG containing an IRF box [61]. In an attempt to identify the conserved regulatory elements, using Ensembl, this sequence was found under "Restricted Elements" in the *IFIH1* promoter in 91 eutherian mammals in position 3′–5′ (online suppl. Fig. 1, 2; for all online suppl. material, see www.karger.com/doi/10.1159/000527008). Moreover, in other distant species such as zebrafish, pigeons, and alligators, in the *Mda5* gene, there is a similar putative regulatory IRF1 sequence showing a strong similarity (Fig. 4e). This sequence is also close to ATG and the flanking sequences do not have any homology between them. These findings suggest a critical role for this IRF sequence in the functional activity of the *Mda5* promoter in humans, mice, and many other different species.

IRF1 Is Critical for Mda5 Induction by IFN-α, LPS, or poly(I:C)

So far, the results allowed us to focus on box 3. Therefore, we tried to find a specific binding sequence corresponding to a transcription factor binding site that could be responsible for the induction of *Mda5* by extra- or intracellular activators. Given the importance of the IRF family of transcription factors in the effects of pro-inflammatory stimuli and the degree of conservation of their binding sequence, we hypothesized that IRF was the key element that was induced and controlled the expression of *Mda5* downstream of extracellular (LPS and IFN-α) and intracellular (poly(I:C)) activators. Deleting the 9 bp of the IRF sequence could interfere with the allosteric structure of the DNA and particularly the DNA-histone interactions, which would introduce an artefact in our experiments. Therefore, we decided to introduce point mutations that changed the consensus IRF-binding sequence. It has been reported that the IRF protein makes contact with DNA through the major groove and interacts with a GAAA motif [62]. Furthermore, most of the conserved base pairs of this binding sequence are two adenosine triplets [63]. Therefore, the conserved adenosine triplets were changed to guanidine, thus producing the mutated sequence GGGGCAGGGG (Fig. 5a). RAW 264.7 cells transfected with the construct carrying specific mutations at the IRF-binding sequence and activated by LPS, IFN-α, or poly(I:C) did not show any luciferase activity (Fig. 5a). Consequently, it can be concluded that the IRF-binding sequence has a critical role in mediating *Mda5* transcription downstream of both external and intracellular stimuli.

Looking in detail at box 3, we observed that between −306 bp and −286 bp, there is a AAGAGAATCGAAACAGAAAC sequence that is a consensus IRF recognition

Fig. 3. *Mda5* expression is stable and the expression is dependent on STAT1. **a** BMDMs were treated with or without IFN-α for 6 h, then DRB (20 g/mL) and actinomycin D (5 g/mL) were added. *Mda5* expression was then measured by RT-PCR at the indicated time points. Cell viability was 95% for all culture conditions. As a control, we also determined the half-life of *c-myc* ($n = 3$). **b** Similar experiment to that in (**a**), but LPS was used instead as the Mda5 activator ($n = 3$). **c** BMDMs from *Stat1* knockout mice and the corresponding wild-type counterparts were isolated and stimulated with IFN-γ, IFN-α, or LPS for 6 h. *Mda5* expression was analyzed by RT-PCR ($n = 4$). **d** Similar experiment to that in (**c**), but using electroporated poly(I:C) as the activator ($n = 4$). **e** Similar experiment to that in (**c**), but using IFN-γ as the activator and analyzing *Ifn-β* expression ($n = 4$). **f** BMDMs were incubated in the presence or not of 5 μg/mL of CHX for 1 h, then IFN-α, LPS, or poly(I:C) was added and incubated for 3 h and *Mda5* was determined ($n = 4$). **g** Similar experiment to that in (**f**), but *Tnf-α* was determined ($n = 4$). Each experiment was performed in triplicate, and the results are shown as the mean ± SD. $^{**}p < 0.01$, $^{***}p < 0.001$, and $p < 0.0001$ in relation to each stimulated sample compared to controls in each experiment. Data were analyzed using the unpaired Student's *t* test.

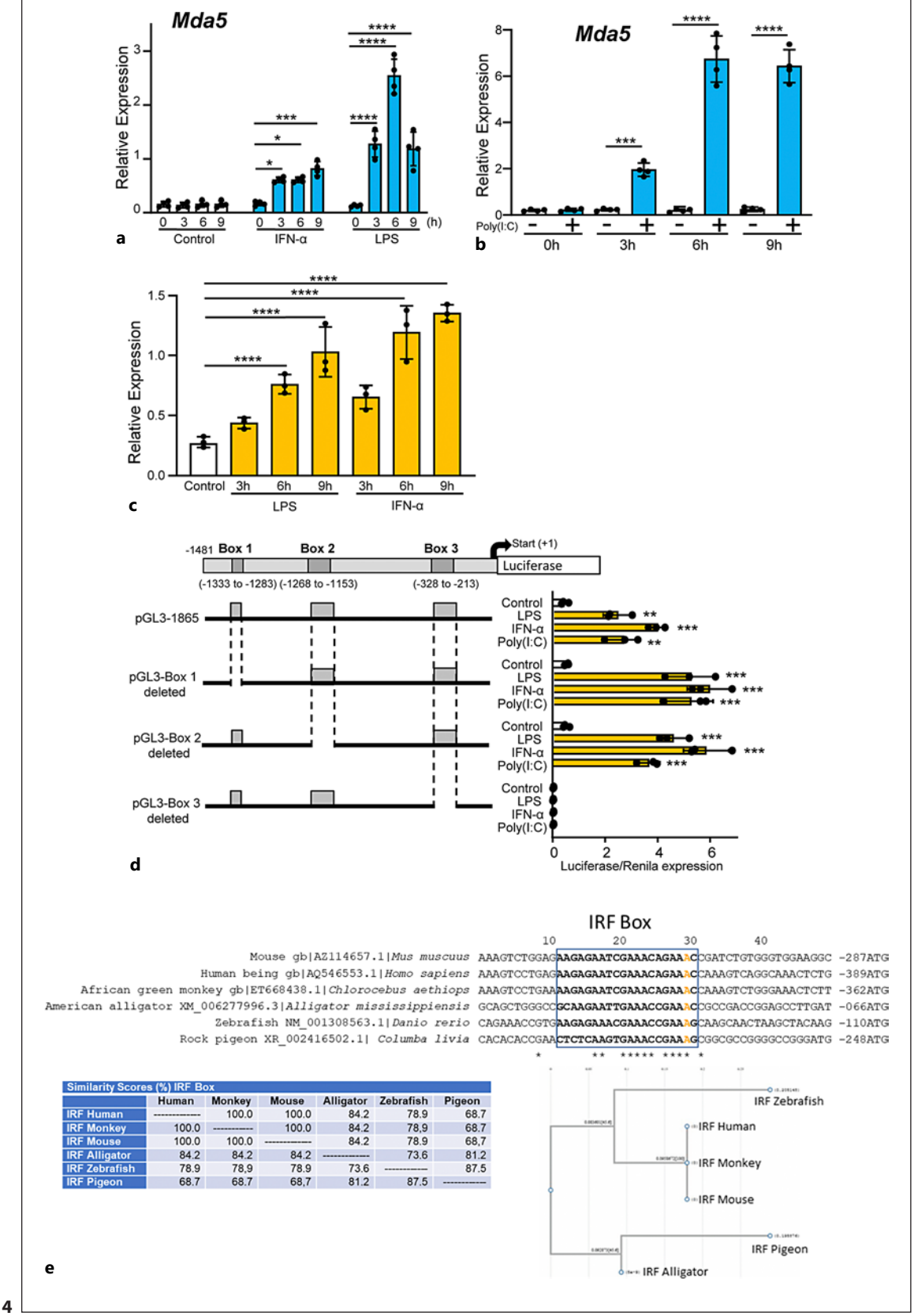

4

(For legend see next page.)

sequence [61]. This indicated the possibility that the IRF protein was required for *Mda5* induction. Among the nine IRFs, five (IRF1, IRF3, IRF7, IRF8, and IRF9) have been implicated as positive regulators of the transcription of type I IFN genes [1]. In fact, the STAT1-dependent nature of IFN-α-, LPS-, or poly(I:C)-stimulated *Mda5* expression (Fig. 3c, d) may be related to the requirement of STAT1 for IRF induction. This observation prompted us to determine the possible involvement of IRF in *Mda5* induction by measuring the time course of expression of these IRFs in response to LPS, IFN-α, or poly(I:C). The only IRF whose induction correlated with that of *Mda5* was *Irf1* (Fig. 5b, c). We have previously shown that after 3 h of IFN-γ treatment IRF1 is synthesized in macrophages [48]. The other four (*Irf3*, *7*, *8*, and *9*) were not induced at 3 h of treatment (Fig. 5d–g). Interestingly, LPS also induces *Irf1* that requires protein synthesis, thereby suggesting that an intermediate product, probably related to type I IFNs, is induced by LPS that then induces *Irf1* expression [48, 64, 65].

IRF1 exerts its effects by directly binding to the promoters of genes [1]. To determine whether IRF1 binds to the *Mda5* promoter, we performed ChIP assays using the −328 bp to −213 bp fragment of the *Mda5* promoter corresponding to box 3. Low levels of amplification were detected in the samples immunoprecipitated using total immunoglobulins. However, increased amplification of the *Mda5* promoter was observed in the sample treated for 3 h (around a 4-fold increase) with IFN-α or LPS and immunoprecipitated with the IRF1-specific antibody (Fig. 6a). The specificity of the reaction was confirmed by using a fragment of the promoter that did not contain the transcription start site (data not shown). This result confirmed that IRF1 binds to the *Mda5* promoter in vivo in response to IFN-α or LPS stimulation.

Here, we show that *Mda5* transcription requires an IRF-binding sequence and that *Irf1* induction by LPS, IFN-α, or poly(I:C) correlates with the initiation of *Mda5* expression. To elucidate the role of IRF1 in *Mda5* induction by both external and intracellular stimuli in BMDMs, we inhibited its expression with siRNA. Under our experimental conditions in which siRNA was transfected by electroporation, we specifically inhibited *Irf1* mRNA expression after induction by IFN-α or LPS (Fig. 6b). Previously, we confirmed this inhibition of IRF1 expression by siRNA treatment through western blots, as well as demonstrating the specificity of this inhibition by showing the noninterference with the expression of *oligoadenylate synthase-1* [48], or with the induction of *Irf3*, *Irf7*, or *Irf9* (online suppl. Fig. 3a–c). IFN-α, LPS, and poly (I:C) induced Mda5 expression in macrophages. However, IRF1 inhibition led to a marked reduction in the expression of *Mda5* (Fig. 6c, d). Similar results were found when we used the RAW 264.7 macrophage cell line (Fig. 6e). These results demonstrated the key role of IRF1 in eliciting *Mda5* expression.

Discussion

In viral RNA infections, MDA5 is a critical sensor of viral RNA, inducing the production of IFN-α and –β [4]. In other diseases where gain-of-function mutations in the *IFIHL* gene are associated with type I interferonopathies such as AGS [31] and autoimmune diseases [35], macrophages may play an important role. In fact, Trex1 and SAMHD1, whose mutations are associated with AGS, are higly expressed in macrophages [48, 66].

Despite MDA5 being a cytosolic sensor of RNA, extracellular activators such as IFN-α/γ and LPS also induce

Fig. 4. Characterization of the Mda5 functional promoter. **a** RAW 264.7 macrophages were incubated for different times with IFN-α or LPS before *Mda5* expression was determined ($n = 4$). **b** Similar experiment to that in (**a**), but using electroporated poly(I:C) as the activator ($n = 4$). **c** RAW 264.7 macrophages were transfected with the pGL3−1481 vector. At 24 h post-transfection, cells were stimulated with LPS or IFN-α for the indicated times before luciferase activity was measured. Controls were nonactivated cells ($n = 4$). **d** Putative consensus binding sites for transcription factors in the *Mda5* gene promoter. The 1481-bp sequence upstream of the *Mda5* transcription start site was analyzed using the JASPAR database. Putative boxes showing more than 85% similarity with the consensus sequence for transcription factor binding sites are shown (boxes 1, 2, and 3). As in (**c**), the vector used contained the indicated deletions of the *Mda5* promoter region. Fold increase in *Mda5* induction by LPS, IFN-α, or poly(I:C) are shown in relation to the untreated cells (Control). Cells were stimulated for 6h. A plasmid encoding the Renilla luciferase under the control of an HSV-TK promoter was co-transfected, with the Renilla luciferase activity used as a control of transfection. Assays are representative of at least three independent experiments showing similar results. Each experiment was performed in triplicate, and the results are shown as the mean ± SD. $^{*}p < 0.05$, $^{**}p < 0.01$, $^{***}p < 0.001$, and $p < 0.0001$ in relation to each stimulated sample compared to controls in each experiment. Data were analyzed using the unpaired Student's *t* test. **e** Sequences alignment of the *Irf1* box in the promoters of *Mda5* in human, mice, monkey, alligator, zebrafish and pigeon. JASPAR and the National center for biotechnology information (NCBI) database were used. For sequences alignment we used the MacVector 18.0. The A in orange indicated the distance to the ATG. In the lower part, the similarity (%) between theses boxes in different species is shown, as well as the phylogram.

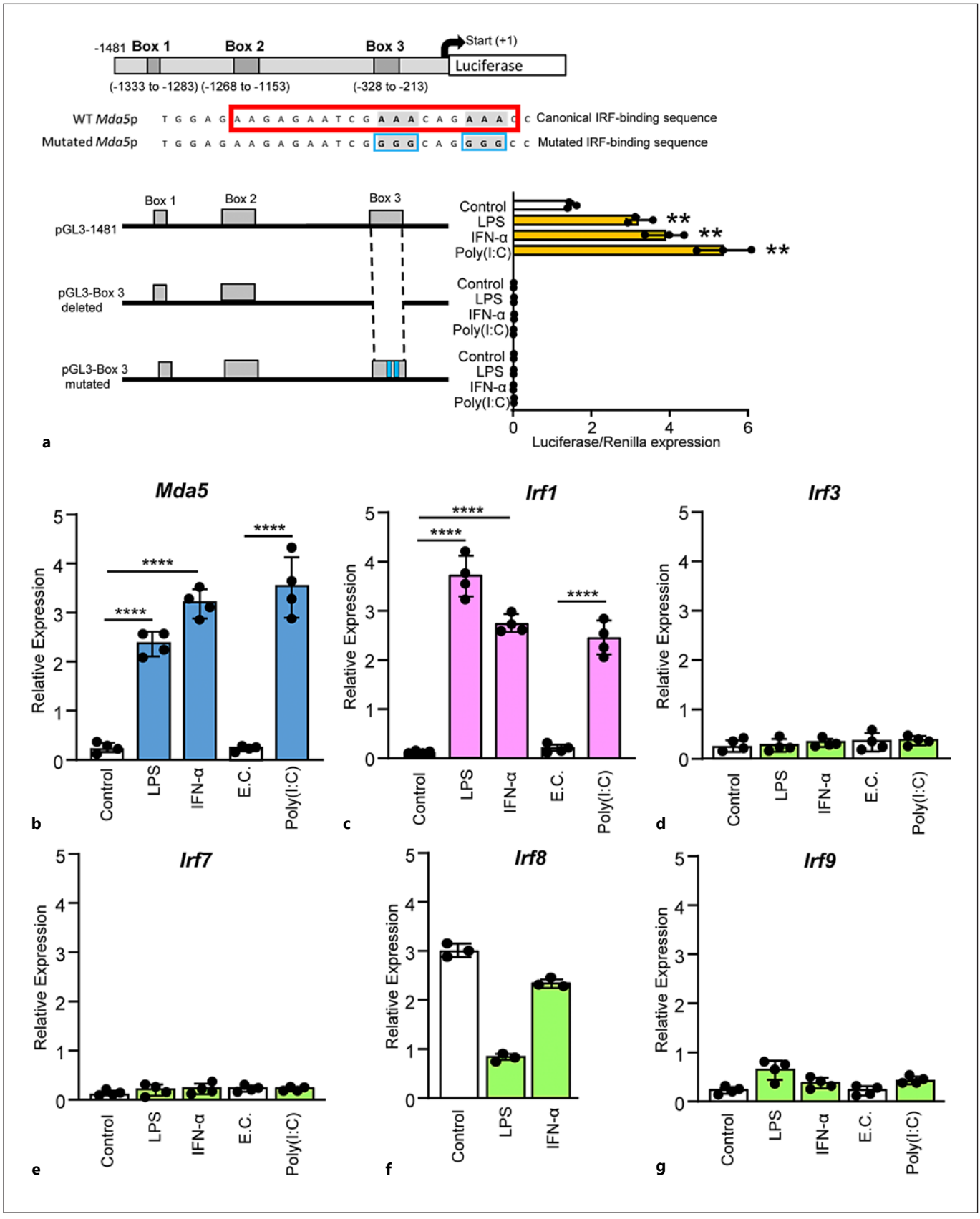

5

(For legend see next page.)

MDA5 expression. Interestingly, we observed that the different activators use a common pathway requiring STAT1. In a recent publication, it was shown that at the early infection stage of some viruses STAT1 can be activated independently of cytokines and JAKs [67] reinforcing the role of STAT1 in virus infections. MDA5, through interactions with MAVS, induces the transcription of the genes encoding type I IFNs [68]. The production of type I IFNs in an autocrine manner enhances the transcription of *Mda5*. The requirement of STAT1 for the activation of *Mda5* expression by LPS was due to a secondary induction of type I IFNs and autocrine signaling through type I IFN receptors [59], as has been described for other genes [58, 59]. Finally, the inhibition of *Mda5* induction by ROS inhibitors was probably related to the need for ROS in type I IFN activation to induce *Mda5* transcription [45].

Since *Mda5* mRNA was very stable before and after IFN-α or LPS treatment and given that increases in mRNA levels could be achieved only through the production of RNA, we concluded that *Mda5* expression in macrophages is regulated at the transcriptional level. Using the JASPAR database, we observed three putative elements in the *Mda5* gene promoter that were responsible for the transcriptional regulation of *Mda5* expression. Through alternating deletions of these elements, we found that only one, which is the closest to the proximal end of the start site, a region located at −328 bp to −213 bp, contains the elements that regulate the *Mda5* expression induced by IFN-α, LPS, or poly(I:C). This region contains a consensus IRF recognition sequence [61].

Interestingly, the AAGAGAATCGAAACAGAAAC sequence that is relatively close to the ATG promoter of the *IFIH1* (*MDA5*) gene is present in 91 eutherian mammals (online suppl. Fig. 1, 2; for all online suppl. material, see Ensembl [105 - Dec 2021 © EMBL-EBI]) and shows a strong similarity in other distant species (Fig. 4e), supporting the hypothesis for a critical role for this IRF sequence in the functional activity of the *Mda5* promoter. All IRFs contain a conserved N-terminal DNA-binding domain, which forms a helix-turn-helix domain with a conserved tryptophan cluster that recognizes DNA sequences [69]. An analysis of the crystal structure of the DNA-binding domain of IRF1 bound to the *Ifnβ* promoter revealed that 5′-GAAA-3′ is the consensus sequence, known as the IRF-element, recognized by the helix-turn-helix motif of IRF1 [62]. All IRFs harbor a C-terminal IRF association domain, which is responsible for homo- and heteromeric interactions with other family members or transcription factors [70].

Irf1, the first member of the IRF family to be identified, targets different sets of genes in various cell types in response to diverse cellular stimuli and evokes appropriate innate and adaptive immune responses [71]. Several lines of evidence demonstrated that IRF1 was necessary for *Mda5* induction including kinetics experiments, ChIP assays, and gene-silencing experiments. Among the four IRFs involved in the positive regulation of the transcription of type I IFN genes [1], the time course of the induction of only IRF1 correlated with that of Mda5. Using bone marrow-derived DCs, it has been described that IRF3, IRF5, and IRF7 expression was MDA5 dependent [13], which could explain its late induction in relation to MDA5 expression. The putative necessity of this protein explains the induction of Mda5 by the different activators starting at around 3 h of treatment as well as the requirement of both STAT1 and protein synthesis. The C-terminal transactivation domain of STAT1 is required for an efficient recruitment of the components of the core Mediator complex to the IRF1 promoter, which harbors an open chromatin state under basal conditions, inducing transcriptional activation [72].

Using ChIP assays, we found that IRF1 binds to the *Mda5* promoter. Moreover, the siRNA experiments demonstrated the key role of IRF1 in *Mda5* transcription. IRF1 has several domains, including an N-terminal DNA-binding domain with 5 characteristically spaced tryptophans and a transactivation domain, as well as a C-terminal regulatory domain involved in the recruitment of coactivators to the IRF1 target promoters [71]. For some IRFs, the regulation of transcriptional activity requires the phosphorylation of serine residues at the C-terminal domain. In this regard, there are reports of IRF1 phosphorylation by casein kinase II that increases the interactions between DNA and protein [73, 74]. The enhancer domain is an important determinant of the rate at which IRF1 is degraded [75].

Fig. 5. IRF1 binding to the *Mda5* promoter is required for *Mda5* transcription. **a** Similar experiment to that in Fig. 4d, but the mutations in the canonical IRF-binding sequence were introduced in box 3. **b–g** In BMDM gene expression was determined by RT-PCR after LPS, IFN-α or poly(I:C) treatment for 3 h with the exception of **f** in which poly(I:C) treatment was not performed. E.C., electroporation control ($n = 4$). **b** *Mda5*, **c** *Irf1*, **d** *Irf3*, **e** *Irf7*, **f** *Irf8*, and **g** *Irf9*. Assays are representative of at least three independent experiments showing similar results. Each experiment was performed in triplicate, and the results are shown as the mean ± SD. $^{**}p < 0.01$ and $p < 0.0001$ in relation to each stimulated sample compared to controls in each experiment. Data were analyzed using the unpaired Student's *t* test.

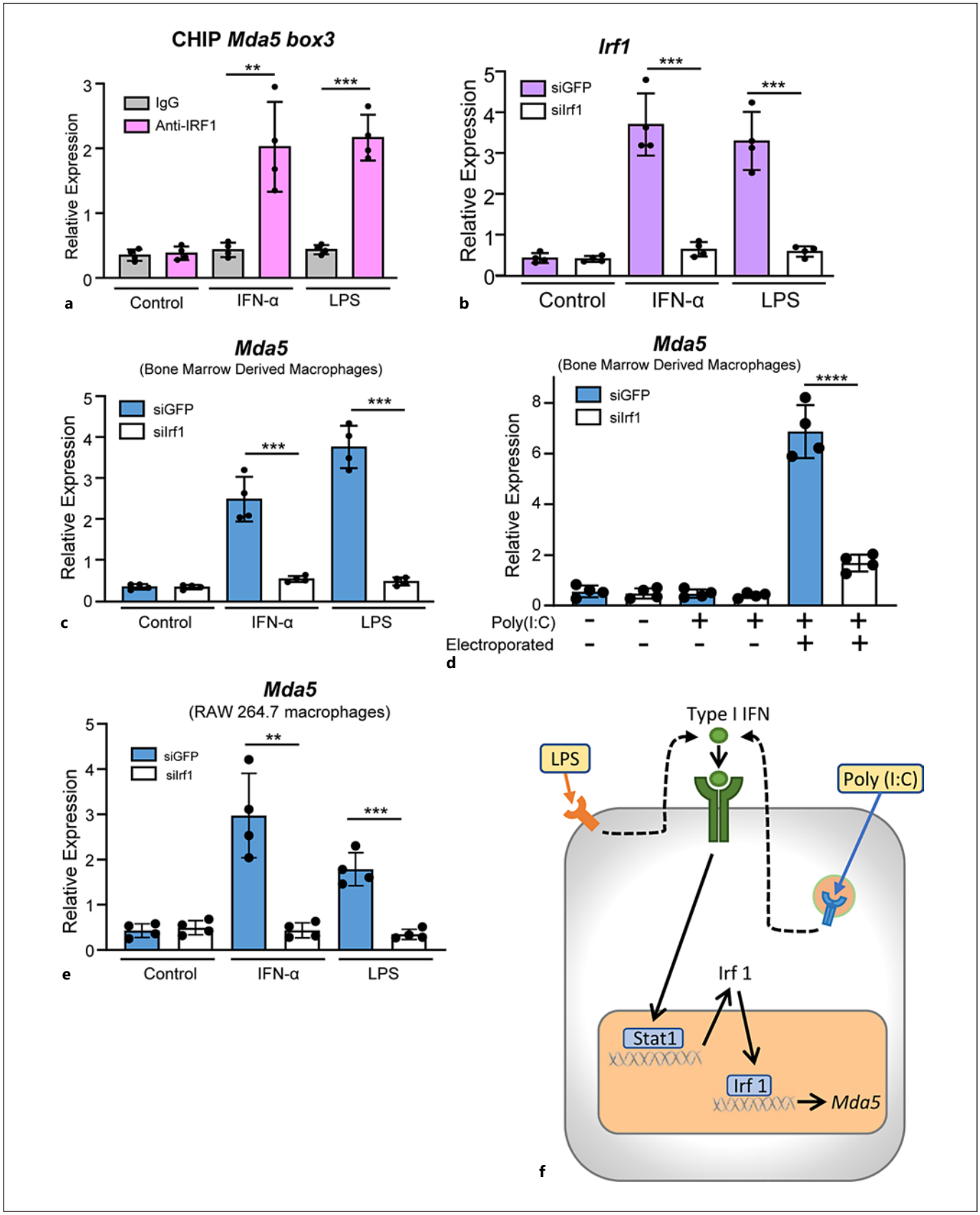

6

(For legend see next page.)

Our results confirmed and extended a previous observation obtained using ChIP and subsequent sequencing (CHIP-Seq) [76]. In mouse macrophages, binding of IRF1 to the IRF box of the *Mda5* promoter was detected, which increased after 2 and 4 h of treatment with LPS (see Gene Expression Omnibus [GEO] database [http://www.ncbi.nlm.nih.gov/gds] under the accession number GSE56123). However, these experiments only indicate that IRF1 bound to the IRF box, whereas in our experiments, in addition to showing the union of IRF1, we demonstrate through mutation of this box the functional activity required for *Mda5* transcription.

Although IRF1 is critical for *Mda5* transcription, we cannot exclude the role of other proteins (enhancers and suppressors) that modulate *Mda5* transcription. Indeed, IRF1 interacts with a number of proteins including transcription factors such as PU.1 and other IRF family members, as well as self-associating through the C-terminal [77, 78].

Finally, we can put forward another possible regulatory mechanism involving histone modifications, which are associated with the recruitment of activators to DNA. In several promoters, STAT1 and IRF1 recruitment to DNA is required for histone acetylation [79]. We did not identify STAT1-binding sites in the *Mda5* promoter. However, it was recently shown that at isolated IRF1 sites lacking STAT1-binding sequences, 25% undergo inducible histone acetylation, 31% exhibit constitutive histone acetylation, and 44% show no histone acetylation (orphan sites) [80]. Interestingly, most isolated IRF1 sites that are constitutively acetylated or undergo inducible acetylation are promoter-proximal, whereas the vast majority of orphan sites are remote. In the human D54MG glioblastoma cell line, IRF1 overexpression leads to the binding of H4Ac and H3K4me3 to *IFIH1* [81], thus suggesting the acetylation of the *Mda5* gene.

In early times (1993–94), it was reported that IRF1 is not essential for the induction of type I IFNs [82, 83]. However, more recently, it has been found that IRF1 plays an important role in viral defense, as shown by ectopic expression of IRF1 that protects otherwise susceptible cells against a diverse range of RNA viruses [84], and IRF1 deficient mice are more susceptible to viral infections [85, 86]. A possible explanation for these contradictory results may be related to the different viruses used in the experiments. Interestingly, RIG-I is essential for the production of IFNs in response to RNA viruses including paramyxoviruses, influenza virus, and Japanese encephalitis virus, whereas MDA5 is critical for picornavirus detection. Furthermore, RIG^{-I-}/ and $MDA5^{-/-}$ mice are highly susceptible to infection with these respective RNA viruses compared to control mice [87]. The different mechanisms for virus recognition and elimination were illustrated with the $IRF1^{-/-}$ mice that were less resistant than normal mice to encephalomyocarditis virus infection, but the absence of IRF1 did not clearly affect replication of two other types of viruses [88].

In summary, we conclude that IRF1 is required under our experimental conditions to induce the expression of Mda5 in macrophages, but we do not exclude that other transcription factors, enhancers, etc., could modulate such expression. We observed a mechanism through which IRF1 controls Mda5 transcription in macrophages (Fig. 6f). This could be important in controlling type I IFN production in viral infections as well as in the development of interferonopathies such as AGS.

Acknowledgments

We acknowledge Dr. Anna Planas (CSIC-IDIBAPS, Spain) for kindly providing the *Stat1* knockout mice.

Statement of Ethics

Animal use was approved by the Animal Research Committee of the University of Barcelona and the Government of Catalunya (approval number 2523).

Fig. 6. IRF1 is required for the induction of *Mda5* in macrophages. **a** In vivo binding of IRF1 to the *Mda5* promoter was analyzed by ChIP assays. Macrophages were treated for 3 h with IFN-α or LPS ($n = 4$). **b** BMDMs were transfected with either an siRNA directed against *Irf1* or a control siRNA against *GFP*. Twenty-four hours after transfection, the cells were stimulated for 3 h with IFN-α or LPS and *Irf1* expression was determined by qPCR ($n = 4$). **c** BMDMs transfected with siRNA against *Irf1* or *GFP* were treated for 3 h with IFN-α or LPS before *Mda5* expression was determined by RT-PCR ($n = 4$). **d** Similar experiment to that in (**c**), but using electroporated poly(I:C) as the activator ($n = 4$). **e** RAW 264.7 macrophage cell line transfected with siRNA against *Irf1* or GFP were treated for 3 h with IFN-α or LPS before *Mda5* expression was determined by RT-PCR ($n = 4$). **f** Schematic representation of the induction of *Mda5* by LPS or IFN-α. Each experiment was performed in triplicate, and the results are shown as the mean ± SD. $^{**}p < 0.01$, $^{***}p < 0.001$, and $p < 0.0001$ in relation to each stimulated sample compared to controls in each experiment. Data were analyzed using the unpaired Student's *t* test.

Conflict of Interest Statement

The authors declare that the research was conducted in the absence of any commercial or financial relationships that could be construed as a potential conflict of interest.

Funding Sources

This work was supported by the Ministerio de Ciencia e Innovación Grant BFU2017-85353 (J.L. and A.C.) and PID2020-1872 1RB-I00 (J.L.).

Author Contributions

Iris Aparicio-Herraiz, Guillem Sánchez-Sánchez, Pere Rehues, Martí López-Serrat, Carlos Batlle, and Lorena Valverde-Estrella performed the experiments and analyzed the data. Jorge Lloberas and Antonio Celada design the study, write the paper, and provide funding support. All the authors contributed to the article and approved the submitted version.

Data Availability Statement

All data generated or analyzed during this study are included in this article and its online supplementary material. Further inquiries can be directed to the corresponding author.

References

1 Honda K, Takaoka A, Taniguchi T. Type I interferon [corrected] gene induction by the interferon regulatory factor family of transcription factors. Immunity. 2006 Sep;25(3):349–60.
2 Yan N, Chen ZJ. Intrinsic antiviral immunity. Nat Immunol. 2012 Feb 16;13(3):214–22.
3 Goubau D, Deddouche S, Reis e Sousa C. Cytosolic sensing of viruses. Immunity. 2013 May 23;38(5):855–69.
4 McNab F, Mayer-Barber K, Sher A, Wack A, O'Garra A. Type I interferons in infectious disease. Nat Rev Immunol. 2015 Feb;15(2):87–103.
5 Solis M, Nakhaei P, Jalalirad M, Lacoste J, Douville R, Arguello M, et al. RIG-I-mediated antiviral signaling is inhibited in HIV-1 infection by a protease-mediated sequestration of RIG-I. J Virol. 2011 Feb;85(3):1224–36.
6 Miller CM, Barrett BS, Chen J, Morrison JH, Radomile C, Santiago ML, et al. Systemic expression of a viral RdRP protects against retrovirus infection and disease. J Virol. 2020 Apr 16;94(9):e00071–20.
7 Liu G, Lee JH, Parker ZM, Acharya D, Chiang JJ, van Gent M, et al. ISG15-dependent activation of the sensor MDA5 is antagonized by the SARS-CoV-2 papain-like protease to evade host innate immunity. Nat Microbiol. 2021 Apr;6(4):467–78.
8 Yin X, Riva L, Pu Y, Martin-Sancho L, Kanamune J, Yamamoto Y, et al. MDA5 governs the innate immune response to SARS-CoV-2 in lung epithelial cells. Cell Rep. 2021 Jan 12;34(2):108628.
9 Gitlin L, Barchet W, Gilfillan S, Cella M, Beutler B, Flavell RA, et al. Essential role of mda-5 in type I IFN responses to polyriboinosinic:polyribocytidylic acid and encephalomyocarditis picornavirus. P Natl Acad Sci USA. 2006 May 30;103(22):8459–64.
10 Francisco E, Suthar M, Gale M Jr, Rosenfeld AB, Racaniello VR. Cell-type specificity and functional redundancy of RIG-I-like receptors in innate immune sensing of Coxsackievirus B3 and encephalomyocarditis virus. Virology. 2019 Feb;528:7–18.
11 McCartney SA, Thackray LB, Gitlin L, Gilfillan S, Virgin HW, Colonna M, et al. MDA-5 recognition of a murine norovirus. PLoS Pathog. 2008 Jul 18;4(7):e1000108.
12 Gitlin L, Benoit L, Song C, Cella M, Gilfillan S, Holtzman MJ, et al. Melanoma differentiation-associated gene 5 (MDA5) is involved in the innate immune response to Paramyxoviridae infection in vivo. PLoS Pathog. 2010 Jan 22;6(1):e1000734.
13 Baños-Lara MDR, Ghosh A, Guerrero-Plata A. Critical role of MDA5 in the interferon response induced by human metapneumovirus infection in dendritic cells and in vivo. J Virol. 2013 Jan;87(2):1242–51.
14 Jin YH, Kim SJ, So EY, Meng L, Colonna M, Kim BS. Melanoma differentiation-associated gene 5 is critical for protection against Theiler's virus-induced demyelinating disease. J Virol. 2012 Feb;86(3):1531–43.
15 Wang Y, Swiecki M, Cella M, Alber G, Schreiber RD, Gilfillan S, et al. Timing and magnitude of type I interferon responses by distinct sensors impact CD8 T cell exhaustion and chronic viral infection. Cell Host Microbe. 2012 Jun 14;11(6):631–42.
16 Brisse M, Huang Q, Rahman M, Di D, Liang Y, Ly H. RIG-I and MDA5 protect mice from Pichinde virus infection by controlling viral replication and regulating immune responses to the infection. Front Immunol. 2021;12:801811.
17 Yu X, Cai B, Wang M, Tan P, Ding X, Wu J, et al. Cross-regulation of two type I interferon signaling pathways in plasmacytoid dendritic cells controls anti-malaria immunity and host mortality. Immunity. 2016 Nov 15;45(5):1093–107.
18 McCartney SA, Vermi W, Lonardi S, Rossini C, Otero K, Calderon B, et al. RNA sensor-induced type I IFN prevents diabetes caused by a beta cell-tropic virus in mice. J Clin Invest. 2011 Apr;121(4):1497–507.
19 Longhi MP, Trumpfheller C, Idoyaga J, Caskey M, Matos I, Kluger C, et al. Dendritic cells require a systemic type I interferon response to mature and induce CD4+ Th1 immunity with poly IC as adjuvant. J Exp Med. 2009 Jul 6;206(7):1589–602.
20 Wang Y, Cella M, Gilfillan S, Colonna M. Cutting edge: polyinosinic:polycytidylic acid boosts the generation of memory CD8 T cells through melanoma differentiation-associated protein 5 expressed in stromal cells. J Immunol. 2010 Mar 15;184(6):2751–5.
21 Barrat FJ, Elkon KB, Fitzgerald KA. Importance of nucleic acid recognition in inflammation and autoimmunity. Ann Rev Med. 2016;67:323–36.
22 Hartmann G. Nucleic Acid Immunity. Adv Immunol. 2017;133:121–69.
23 Zhao C, Jia M, Song H, Yu Z, Wang W, Li Q, et al. The E3 ubiquitin ligase TRIM40 attenuates antiviral immune responses by targeting MDA5 and RIG-I. Cell Rep. 2017 Nov 7;21(6):1613–23.
24 Wies E, Wang MK, Maharaj NP, Chen K, Zhou S, Finberg RW, et al. Dephosphorylation of the RNA sensors RIG-I and MDA5 by the phosphatase PP1 is essential for innate immune signaling. Immunity. 2013 Mar 21;38(3):437–49.
25 Davis ME, Wang MK, Rennick LJ, Full F, Gableske S, Mesman AW, et al. Antagonism of the phosphatase PP1 by the measles virus V protein is required for innate immune escape of MDA5. Cell Host Microbe. 2014 Jul 9;16(1):19–30.
26 Takashima K, Oshiumi H, Takaki H, Matsumoto M, Seya T. RIOK3-mediated phosphorylation of MDA5 interferes with its assembly and attenuates the innate immune response. Cell Rep. 2015 Apr 14;11(2):192–200.
27 Lee NR, Kim HI, Choi MS, Yi CM, Inn KS. Regulation of MDA5-MAVS antiviral signaling axis by TRIM25 through TRAF6-mediated NF-κB activation. Mol Cells. 2015 Sep;38(9):759–64.

28 Orzalli MH, Kagan JC. Apoptosis and necroptosis as host defense strategies to prevent viral infection. Trends Cell Biol. 2017 Nov;27(11):800–9.
29 Crow YJ, Manel N. Aicardi-Goutieres syndrome and the type I interferonopathies. Nat Rev Immunol. 2015 Jul;15(7):429–40.
30 Pereira-Lopes S, Tur J, Calatayud-Subias JA, Lloberas J, Stracker TH, Celada A. NBS1 is required for macrophage homeostasis and functional activity in mice. Blood. 2015 Nov 26;126(22):2502–10.
31 Rice GI, Del Toro Duany Y, Jenkinson EM, Forte GM, Anderson BH, Ariaudo G, et al. Gain-of-function mutations in IFIH1 cause a spectrum of human disease phenotypes associated with upregulated type I interferon signaling. Nat Genet. 2014 May;46(5):503–9.
32 Oda H, Nakagawa K, Abe J, Awaya T, Funabiki M, Hijikata A, et al. Aicardi-Goutieres syndrome is caused by IFIH1 mutations. Am J Hum Genet. 2014 Jul 3;95(1):121–5.
33 Domsgen E, Lind K, Kong L, Huhn MH, Rasool O, van Kuppeveld F, et al. An IFIH1 gene polymorphism associated with risk for autoimmunity regulates canonical antiviral defence pathways in Coxsackievirus infected human pancreatic islets. Sci Rep. 2016 Dec 21;6:39378.
34 Sadler AJ. The role of MDA5 in the development of autoimmune disease. J Leuk Biol. 2018 Feb;103(2):185–92.
35 Dias Junior AG, Sampaio NG, Rehwinkel J. A balancing act: MDA5 in antiviral immunity and Autoinflammation. Trends Microbiol. 2019 Jan;27(1):75–85.
36 Funabiki M, Kato H, Miyachi Y, Toki H, Motegi H, Inoue M, et al. Autoimmune disorders associated with gain of function of the intracellular sensor MDA5. Immunity. 2014 Feb 20;40(2):199–212.
37 Gorman JA, Hundhausen C, Errett JS, Stone AE, Allenspach EJ, Ge Y, et al. The A946T variant of the RNA sensor IFIH1 mediates an interferon program that limits viral infection but increases the risk for autoimmunity. Nat Immunol. 2017 Jul;18(7):744–52.
38 Chiappinelli KB, Strissel PL, Desrichard A, Li H, Henke C, Akman B, et al. Inhibiting DNA methylation causes an interferon response in cancer via dsRNA including endogenous retroviruses. Cell. 2015 Aug 27;162(5):974–86.
39 Roulois D, Loo Yau H, Singhania R, Wang Y, Danesh A, Shen SY, et al. DNA-demethylating agents target colorectal cancer cells by inducing viral mimicry by endogenous transcripts. Cell. 2015 Aug 27;162(5):961–73.
40 Dhir A, Dhir S, Borowski LS, Jimenez L, Teitell M, Rotig A, et al. Mitochondrial double-stranded RNA triggers antiviral signalling in humans. Nature. 2018 Aug;560(7717):238–42.
41 Quicke KM, Diamond MS, Suthar MS. Negative regulators of the RIG-I-like receptor signaling pathway. Eur J Immunol. 2017 Apr;47(4):615–28.
42 Celada A, Gray PW, Rinderknecht E, Schreiber RD. Evidence for a gamma-interferon receptor that regulates macrophage tumoricidal activity. J Exp Med. 1984 Jul 1;160(1):55–74.
43 Meraz MA, White JM, Sheehan KC, Bach EA, Rodig SJ, Dighe AS, et al. Targeted disruption of the Stat1 gene in mice reveals unexpected physiologic specificity in the JAK-STAT signaling pathway. Cell. 1996 Feb 9;84(3):431–42.
44 Sebastian C, Serra M, Yeramian A, Serrat N, Lloberas J, Celada A. Deacetylase activity is required for STAT5-dependent GM-CSF functional activity in macrophages and differentiation to dendritic cells. J Immunol. 2008 May 1;180(9):5898–906.
45 Tur J, Pereira-Lopes S, Vico T, Marin EA, Munoz JP, Hernandez-Alvarez M, et al. Mitofusin 2 in macrophages links mitochondrial ROS production, cytokine release, phagocytosis, autophagy, and bactericidal activity. Cell Rep. 2020 Aug 25;32(8):108079.
46 Bustin SA, Benes V, Garson JA, Hellemans J, Huggett J, Kubista M, et al. The MIQE guidelines: minimum information for publication of quantitative real-time PCR experiments. Clin Chem. 2009 Apr;55(4):611–22.
47 Hellemans J, Mortier G, De Paepe A, Speleman F, Vandesompele J. qBase relative quantification framework and software for management and automated analysis of real-time quantitative PCR data. Genome Biol. 2007;8(2):R19.
48 Valverde-Estrella L, Lopez-Serrat M, Sanchez-Sanchez G, Vico T, Lloberas J, Celada A. Induction of Samhd1 by interferon gamma and lipopolysaccharide in murine macrophages requires IRF1. Eur J Immunol. 2020 Sep;50(9):1321–34.
49 Sebastian C, Herrero C, Serra M, Lloberas J, Blasco MA, Celada A. Telomere shortening and oxidative stress in aged macrophages results in impaired STAT5a phosphorylation. J Immunol. 2009 Aug 15;183(4):2356–64.
50 Saitou N, Nei M. The neighbor-joining method: a new method for reconstructing phylogenetic trees. Mol Biol Evol. 1987 Jul;4(4):406–25.
51 Kumar S, Stecher G, Li M, Knyaz C, Tamura K. MEGA X: Molecular Evolutionary Genetics Analysis across computing platforms. Mol Biol Evol. 2018 Jun 1;35(6):1547–9.
52 Yeramian A, Martin L, Serrat N, Arpa L, Soler C, Bertran J, et al. Arginine transport via cationic amino acid transporter 2 plays a critical regulatory role in classical or alternative activation of macrophages. J Immunol. 2006 May 15;176(10):5918–24.
53 Pujantell M, Riveira-Munoz E, Badia R, Castellvi M, Garcia-Vidal E, Sirera G, et al. RNA editing by ADAR1 regulates innate and antiviral immune functions in primary macrophages. Sci Rep. 2017 Oct 17;7(1):13339.
54 Matsumoto M, Seya T. TLR3: interferon induction by double-stranded RNA including poly(I:C). Adv Drug Deliver Rev. 2008 Apr 29;60(7):805–12.
55 Wornle M, Sauter M, Kastenmuller K, Ribeiro A, Roeder M, Schmid H, et al. Novel role of toll-like receptor 3, RIG-I and MDA5 in poly (I:C) RNA-induced mesothelial inflammation. Mol Cell Biochem. 2009 Feb;322(1–2):193–206.
56 Celada A, Klemsz MJ, Maki RA. Interferon-gamma activates multiple pathways to regulate the expression of the genes for major histocompatibility class II I-A beta, tumor necrosis factor and complement component C3 in mouse macrophages. Eur J Immunol. 1989 Jun;19(6):1103–9.
57 Casals C, Barrachina M, Serra M, Lloberas J, Celada A. Lipopolysaccharide up-regulates MHC class II expression on dendritic cells through an AP-1 enhancer without affecting the levels of CIITA. J Immunol. 2007 May 15;178(10):6307–15.
58 Marques L, Brucet M, Lloberas J, Celada A. STAT1 regulates lipopolysaccharide- and TNF-alpha-dependent expression of transporter associated with antigen processing 1 and low molecular mass polypeptide 2 genes in macrophages by distinct mechanisms. J Immunol. 2004 Jul 15;173(2):1103–10.
59 Sheikh F, Dickensheets H, Gamero AM, Vogel SN, Donnelly RP. An essential role for IFN-beta in the induction of IFN-stimulated gene expression by LPS in macrophages. J Leuk Biol. 2014 Oct;96(4):591–600.
60 O'Neill LAJ, Bowie AG. The family of five: TIR-domain-containing adaptors in Toll-like receptor signalling. Nat Rev Immunol. 2007 May;7(5):353–64.
61 Fujii Y, Shimizu T, Kusumoto M, Kyogoku Y, Taniguchi T, Hakoshima T. Crystal structure of an IRF-DNA complex reveals novel DNA recognition and cooperative binding to a tandem repeat of core sequences. EMBO J. 1999 Sep 15;18(18):5028–41.
62 Escalante CR, Yie J, Thanos D, Aggarwal AK. Structure of IRF-1 with bound DNA reveals determinants of interferon regulation. Nature. 1998 Jan 1;391(6662):103–6.
63 Tanaka N, Kawakami T, Taniguchi T. Recognition DNA sequences of interferon regulatory factor 1 (IRF-1) and IRF-2, regulators of cell growth and the interferon system. Mol Cell Biol. 1993 Aug;13(8):4531–8.
64 Gao JJ, Filla MB, Fultz MJ, Vogel SN, Russell SW, Murphy WJ. Autocrine/paracrine IFN-alphabeta mediates the lipopolysaccharide-induced activation of transcription factor Stat1alpha in mouse macrophages: pivotal role of Stat1alpha in induction of the inducible nitric oxide synthase gene. J Immunol. 1998 Nov 1;161(9):4803–10.
65 Liang HPH, Kerschen EJ, Hernandez I, Basu S, Zogg M, Botros F, et al. EPCR-dependent PAR2 activation by the blood coagulation initiation complex regulates LPS-triggered interferon responses in mice. Blood. 2015 Apr 30;125(18):2845–54.

66 Serra M, Forcales SV, Pereira-Lopes S, Lloberas J, Celada A. Characterization of Trex1 induction by IFN-gamma in murine macrophages. J Immunol. 2011 Feb 15;186(4):2299–308.
67 Liu S, Liao Y, Chen B, Chen Y, Yu Z, Wei H, et al. Critical role of Syk-dependent STAT1 activation in innate antiviral immunity. Cell Rep. 2021 Jan 19;34(3):108627.
68 Mesev EV, LeDesma RA, Ploss A. Decoding type I and III interferon signalling during viral infection. Nat Microbiol. 2019 Jun;4(6):914–24.
69 Honda K, Taniguchi T. IRFs: master regulators of signalling by Toll-like receptors and cytosolic pattern-recognition receptors. Nat Rev Immunol. 2006 Sep;6(9):644–58.
70 Taniguchi T, Ogasawara K, Takaoka A, Tanaka N. IRF family of transcription factors as regulators of host defense. Ann Rev Immunol. 2001;19:623–55.
71 Platanitis E, Decker T. Regulatory networks involving STATs, IRFs, and NFκB in inflammation. Front Immunol. 2018;9:2542.
72 Parrini M, Meissl K, Ola MJ, Lederer T, Puga A, Wienerroither S, et al. The C-terminal transactivation domain of STAT1 has a gene-specific role in transactivation and cofactor recruitment. Front Immunol. 2018;9:2879.
73 Sharf R, Meraro D, Azriel A, Thornton AM, Ozato K, Petricoin EF, et al. Phosphorylation events modulate the ability of interferon consensus sequence binding protein to interact with interferon regulatory factors and to bind DNA. J Biol Chem. 1997 Apr 11;272(15):9785–92.
74 Lin R, Hiscott J. A role for casein kinase II phosphorylation in the regulation of IRF-1 transcriptional activity. Mol Cell Biochem. 1999 Jan;191(1–2):169–80.
75 Pion E, Narayan V, Eckert M, Ball KL. Role of the IRF-1 enhancer domain in signalling polyubiquitination and degradation. Cell Signal. 2009 Oct;21(10):1479–87.
76 Mancino A, Termanini A, Barozzi I, Ghisletti S, Ostuni R, Prosperini E, et al. A dual cis-regulatory code links IRF8 to constitutive and inducible gene expression in macrophages. Genes Dev. 2015 Feb 15;29(4):394–408.
77 Wang IM, Blanco JC, Tsai SY, Tsai MJ, Ozato K. Interferon regulatory factors and TFIIB cooperatively regulate interferon-responsive promoter activity in vivo and in vitro. Mol Cell Biol. 1996 Nov;16(11):6313–24.
78 Meraro D, Hashmueli S, Koren B, Azriel A, Oumard A, Kirchhoff S, et al. Protein-protein and DNA-protein interactions affect the activity of lymphoid-specific IFN regulatory factors. J Immunol. 1999 Dec 15;163(12):6468–78.
79 Ramsauer K, Farlik M, Zupkovitz G, Seiser C, Kroger A, Hauser H, et al. Distinct modes of action applied by transcription factors STAT1 and IRF1 to initiate transcription of the IFN-gamma-inducible gbp2 gene. P Natl Acad Sci USA. 2007 Feb 20;104(8):2849–54.
80 Abou El Hassan M, Huang K, Xu Z, Yu T, Bremner R. Frequent interferon regulatory factor 1 (IRF1) binding at remote elements without histone modification. J Biol Chem. 2018 Jun 29;293(26):10353–62.
81 Zhang Z, Shi L, Song L, Ephrem E, Petri M, Sullivan KE. Interferon regulatory factor 1 marks activated genes and can induce target gene expression in systemic lupus erythematosus. Arthritis Rheumatol. 2015 Mar;67(3):785–96.
82 Ruffner H, Reis LF, Naf D, Weissmann C. Induction of type I interferon genes and interferon-inducible genes in embryonal stem cells devoid of interferon regulatory factor 1. P Natl Acad Sci U S A. 1993 Dec 15;90(24):11503–7.
83 Reis LF, Ruffner H, Stark G, Aguet M, Weissmann C. Mice devoid of interferon regulatory factor 1 (IRF-1) show normal expression of type I interferon genes. EMBO J. 1994 Oct 17;13(20):4798–806.
84 Schoggins JW, Wilson SJ, Panis M, Murphy MY, Jones CT, Bieniasz P, et al. A diverse range of gene products are effectors of the type I interferon antiviral response. Nature. 2011 Apr 28;472(7344):481–5.
85 Maloney NS, Thackray LB, Goel G, Hwang S, Duan E, Vachharajani P, et al. Essential cell-autonomous role for interferon (IFN) regulatory factor 1 in IFN-gamma-mediated inhibition of norovirus replication in macrophages. J Virol. 2012 Dec;86(23):12655–64.
86 Mboko WP, Mounce BC, Emmer J, Darrah E, Patel SB, Tarakanova VL. Interferon regulatory factor 1 restricts gammaherpesvirus replication in primary immune cells. J Virol. 2014 Jun;88(12):6993–7004.
87 Kato H, Takeuchi O, Sato S, Yoneyama M, Yamamoto M, Matsui K, et al. Differential roles of MDA5 and RIG-I helicases in the recognition of RNA viruses. Nature. 2006 May 4;441(7089):101–5.
88 Kimura T, Nakayama K, Penninger J, Kitagawa M, Harada H, Matsuyama T, et al. Involvement of the IRF-1 transcription factor in antiviral responses to interferons. Science. 1994 Jun 24;264(5167):1921–4.